

**UNCLASSIFIED**

**AD 431533**

**DEFENSE DOCUMENTATION CENTER**

FOR

**SCIENTIFIC AND TECHNICAL INFORMATION**

CAMERON STATION, ALEXANDRIA, VIRGINIA



**UNCLASSIFIED**

**NOTICE:** When government or other drawings, specifications or other data are used for any purpose other than in connection with a definitely related government procurement operation, the U. S. Government thereby incurs no responsibility, nor any obligation whatsoever; and the fact that the Government may have formulated, furnished, or in any way supplied the said drawings, specifications, or other data is not to be regarded by implication or otherwise as in any manner licensing the holder or any other person or corporation, or conveying any rights or permission to manufacture, use or sell any patented invention that may in any way be related thereto.



THE INFLUENCE OF SLIGHT LEADING-EDGE BLUNTNESS  
ON BOUNDARY-LAYER TRANSITION  
AT A MACH NUMBER OF EIGHT

By

Jack D. Whitfield and J. Leith Potter  
von Kármán Gas Dynamics Facility  
ARO, Inc.

a subsidiary of Sverdrup and Parcel, Inc.

March 1964

ARO Project No. VB2943

**ABSTRACT**

The influence of leading-edge geometry on boundary-layer transition on a hollow cylinder aligned with the flow has been studied under hypersonic conditions with near adiabatic wall temperature. Effects on the Reynolds number of boundary-layer transition produced by varying free-stream unit Reynolds number and small degrees of leading-edge bluntness are shown to be qualitatively similar to results previously reported by the authors for Mach numbers of 3 to 5. There was a pronounced favorable effect associated with increases in both factors.

Comparisons are made with the theoretical estimates of the influence of bluntness given by Moeckel. Although qualitative agreement with Moeckel's theory is noted, quantitative agreement is not shown and some doubt concerning the theory is expressed.

**PUBLICATION REVIEW**

This report has been reviewed and publication is approved.



Jay T. Edwards, III  
Capt, USAF  
Gas Dynamics Division  
DCS/Research



Donald R. Eastman, Jr.  
DCS/Research

## CONTENTS

	<u>Page</u>
ABSTRACT . . . . .	iii
NOMENCLATURE . . . . .	vii
1.0 INTRODUCTION . . . . .	1
2.0 EXPERIMENTAL APPARATUS	
2.1 Wind Tunnel . . . . .	2
2.2 Model and Instrumentation . . . . .	2
3.0 RESULTS AND DISCUSSION	
3.1 Location of Transition . . . . .	3
3.2 Effect of Leading-Edge Geometry . . . . .	4
3.3 Influence of Mach Number on the Effect of Bluntness . . . . .	6
4.0 CONCLUDING REMARKS . . . . .	8
REFERENCES . . . . .	9

## ILLUSTRATIONS

Figure

1. Typical Models	
a. The 6-in.-diam, Hollow Cylinder Model . . . . .	11
b. Enlarged Photograph of Cross Section of Typical Model Leading Edge . . . . .	11
2. Typical Data Showing Location of Boundary-Layer Transition on Hollow Cylinder at $M_\infty = 8$ . . . . .	12
3. Reynolds Number of Transition on Hollow Cylinder at $M_\infty = 8$ with $b = 0.0006$ in. and $\bar{\theta} = 12.5$ deg . . . . .	13
4. Basic Data Showing $Re_t$ as a Function of $U_\infty/v_\infty$ and $b$ for $M_\infty = 8$ and $\bar{\theta} = 12.5$ deg . . . . .	14
5. Basic Data Showing $Re_t$ as a Function of $U_\infty/v_\infty$ and $b$ for $M_\infty = 8$ and $\bar{\theta} = 5.6$ deg . . . . .	15
6. Bluntness Reynolds Number Influence for Various Unit Reynolds Numbers . . . . .	16
7. Unit Reynolds Number Effect for Various Mach Numbers as $Re_b \rightarrow 0$ . . . . .	17
8. Transition Reynolds Number Increase as a Function of Bluntness Reynolds Number . . . . .	18

<u>Figure</u>		<u>Page</u>
9.	Comparison of Experiment and Theory for Mach Number Influence on Bluntness Effect	
	a. $U_{\infty}/\nu_{\infty} = 10^5 \text{ in.}^{-1}$ . . . . .	19
	b. $U_{\infty}/\nu_{\infty} = 3 \times 10^5 \text{ in.}^{-1}$ . . . . .	20

## NOMENCLATURE

a	Cylinder radius
b	Leading-edge thickness (Fig. 1)
f	"Function of"
M	Mach number
p	Pressure
p(x)	Pitot pressure measured by probe moved along body surface
Re <sub>b</sub>	Bluntness Reynolds number, $U_{\infty} b / \nu_{\infty}$
Re <sub>t</sub>	Transition Reynolds number, $U_{\infty} x_t / \nu_{\infty}$
Re <sub>t, b=0</sub>	Value of Re <sub>t</sub> obtained by extrapolation to b = 0 condition
$\Delta Re_t$	Re <sub>t</sub> - Re <sub>t, b=0</sub>
T	Temperature
U	Velocity
x	Longitudinal, wetted distance from leading edge of body
x <sub>t</sub>	Location of transition as defined by maximum measured p (x)
Y <sub>c</sub>	Height above surface where maximum fluctuation energy is indicated (see "critical height", Ref. 1.)
Y <sub>n</sub>	Thickness of inviscid shear layer associated with the fluid passing between the stagnation streamline and the sonic point of the nose shock wave on blunted bodies
y	Distance measured normal to surface, zero on surface
$\delta$	Boundary-layer thickness
$\delta^*$	Boundary-layer displacement thickness
$\theta$	Bevel angle of lower or interior leading edge (see Fig. 1)
$\bar{\theta}$	Mean value of $\theta$ for all noses of a set having a nominal value of $\theta$

**SUBSCRIPTS**

aw	Adiabatic wall value
n	Ideal, inviscid, body surface value
o	Total or isentropic stagnation value
t	Evaluated at beginning of transition (except $x_t$ )
w	Wall value
$\infty$	Free-stream value

## 1.0 INTRODUCTION

In earlier papers (Refs. 1 and 2) the authors presented discussions of the subject, including extensive experimental data for a Mach number of approximately three. Because of the interest in boundary-layer transition in hypersonic flows, it was believed worthwhile to extend the earlier studies to determine the results for a higher Mach number. The present report concerns the influence of slight leading-edge bluntness on the location of boundary-layer transition on the surface of a hollow cylinder with its major axis parallel to a stream at a Mach number of eight. Earlier investigations have shown this configuration to be equivalent to a flat plate when boundary-layer thickness,  $\delta$ , is small compared to cylinder radius,  $a$ . Although  $\delta/a$  became as large as 0.14 prior to transition in the present case, the departure from essentially flat-plate flow is not believed serious. The effect of this value of  $\delta/a$  increased momentum thickness less than one percent above the flat-plate value according to a calculation based on Ref. 3.

Perhaps it is desirable to attempt to define the term "slight bluntness." For present purposes it is believed sufficient to stipulate that thickness of the leading edge,  $b$ , and the wetted length from the stagnation point to the beginning of transition,  $x_t$ , are related such that  $x_t \gg b$  or, say,  $x_t/b = 0(100)$  or greater. All the data considered in Refs. 1 and 2 and the present report correspond to  $x_t/b = 0(1000)$ .

The importance of slight leading-edge bluntness in connection with transition location, which had been suggested earlier, was further verified in Refs. 1 and 2, where it was shown that changing the thickness of the leading edge from, say, 0.0015 in. to 0.0030 in. could result in the Reynolds number of transition increasing by 355,000, or more than twenty percent in a typical case. The models on which these effects were noted were either flat plates or hollow cylinders, both parallel to the flow direction.

Based on study of data from a number of sources, in Ref. 1 a correlation of available data was achieved. Because the available data corresponded to Mach numbers of 3 to 5 and a large effect of both leading-edge geometry and Mach number was indicated, an investigation with the Mach number equal to 8 promised to reveal information of value in designing and testing hypersonic wings and fins.

---

Manuscript received January 1964.

A qualitatively similar effect of bluntness on conical models has been demonstrated by the work of Rogers (Ref. 4) and Brinich and Sands (Ref. 5). In the latter reference, which also includes data on hollow cylinders, the influence of several different types of bluntness was compared and found to be important.

Like the previous work (Refs. 1 and 2), this research was conducted in the von Kármán Gas Dynamics Facility (VKF), Arnold Engineering Development Center (AEDC), Air Force Systems Command (AFSC).

## 2.0 EXPERIMENTAL APPARATUS

### 2.1 WIND TUNNEL

The 50-in. -diam Mach 8 hypersonic wind tunnel (Gas Dynamic Wind Tunnel, Hypersonic (B)) (Ref. 6) of the VKF was utilized for the experimental studies. This tunnel is of the continuous-flow type and is equipped with a contoured axisymmetric nozzle for a Mach number of 8. Reservoir stagnation pressures from 60 to 800 psia were available, and the reservoir temperature was maintained at about 1335 °R, which is sufficient, even without supercooling, to avoid possible air liquefaction. The 6-in. -diam hollow cylinder model described below was mounted in a flow field which was uniform in Mach number to about  $\pm 0.3$  percent. Because of changes in boundary-layer thickness on the nozzle wall caused by changing pressure level, the average Mach number varied from about 8.0 at a reservoir pressure of 100 psia to about 8.1 at a reservoir pressure of 800 psia. Radiant heat losses from the test model to the water-cooled nozzle walls produced equilibrium model surface temperatures less than the adiabatic value. Variations in the convective heat-transfer rate with pressure level result, of course, in equilibrium model surface temperature variations with pressure level. Typically, model temperatures near the end of the laminar flow region varied from 830°R at a reservoir pressure of 100 psia to 930°R at a reservoir pressure of 800 psia.

### 2.2 MODEL AND INSTRUMENTATION

The test model was a 6-in. -diam hollow cylinder (Fig. 1a), and measurements were taken on the exterior surface. The model was instrumented with 41 surface thermocouples and 12 static-pressure taps imbedded in hot-sprayed aluminum oxide. The relative porosity of the aluminum oxide makes an accurate estimate of the surface finish difficult. Conventional machine shop practice will produce readings

of 100 to 200  $\mu$  in. rms. However, comparisons of transition locations on this model with a much smoother ( $\approx 10 \mu$  in. rms) stainless steel hollow cylinder agree, as previously reported in Ref. 1, indicating that the aluminum-oxide-coated cylinder is aerodynamically smooth for the present test conditions. It should be noted that the hollow cylinder used here differs from the 6-in. -diam hollow cylinder previously described in Ref. 1 only by the addition of a 12-in. -long extension between the interchangeable noses and the instrumented segment of the cylinder.

Six interchangeable noses (Fig. 1a) were used in this study. Two noses had an internal bevel angle of  $5.6 \pm 0.5$  deg and leading-edge thicknesses of 0.0032 and 0.0064 in. Four noses had an internal bevel angle of  $12.5 \pm 0.5$  deg and leading-edge thicknesses of 0.0006, 0.0034, 0.0067, and 0.0094 in., respectively. The leading-edge thickness of the sharper,  $b = 0.0006$  in.,  $\bar{\theta} = 12.5$ -deg nose was erroneously given in Refs. 1 and 2 as 0.002 in. Fortunately, data from this nose were not used in the analysis of bluntness in Refs. 1 and 2. Measurements of the interchangeable noses used here were accomplished in a non-destructive manner by making molds of the leading edges using General Electric Company RTV 60 silicone rubber compound. The resulting doughnut-shaped molds were cut into segments approximately 0.02- to 0.08-in. thick normal to the model leading edges at various circumferential positions. Measurements of magnified images of the molds of the leading edges under a microscope were found to be reproducible within  $\pm 0.0001$  in. for the leading-edge thickness and within  $\pm 0.08$  deg for the lower bevel angles. Figure 1b is an enlarged photograph of one of the moldings of a cross section of nose N<sub>3A</sub>. The images which were measured were somewhat larger.

The model surface temperatures and static pressures were obtained with conventional wind tunnel instrumentation. A remotely controlled traversing and rotating probe mechanism was used to obtain the longitudinal and lateral pitot-pressure profiles. An 0.06-in. -OD pitot-pressure probe was used. In obtaining  $p(x)$ , the pitot pressure distribution along the surface of the model, the probe was traversed in such a manner that  $y/\delta$  was approximately constant as  $x$  varied.

### 3.0 RESULTS AND DISCUSSION

#### 3.1 LOCATION OF TRANSITION

Typical data are shown in Fig. 2 where  $T_w/T_o$ ,  $\delta/x$ , and  $p(x)/p_o$  are plotted as functions of  $x$ . It is interesting to note the considerable

length between the beginning of transition and its end as indicated by the variation of any of the three functions of  $x$  shown in Fig. 2.

It is evident in Fig. 2 that model surface temperatures are not the adiabatic wall values. This was mainly due to radiation cooling,  $T_0$  being 1335°R in most cases, and  $T_w/T_0$  varied with total pressure in the expected fashion. Apparently wall temperature did not vary widely enough run to run to produce a significant effect on transition location, although there was an effect on boundary-layer thickness.

In Fig. 3 the values of  $Re_t$  corresponding to beginning and end of transition are plotted as functions of  $(U/\nu)_\infty$ . For this purpose, the beginning has been taken as that station where  $\delta/x^{0.5}$  departs from a constant value at a fixed  $(U/\nu)_\infty$ , and the end of transition has been taken as that station where  $\delta/x^{0.8}$  attains a constant value. Maximum values of  $T_w/T_0$  and  $p(x)/p_0$  are identifiable in the data (see Fig. 2) and may also be used to locate transition. However, as shown in Figs. 2 and 3, the peak values of  $T_w/T_0$  and  $p(x)/p_0$  appear to lie between the extremities of the transition region bounded by the laminar and turbulent forms of  $\delta(x)$ . Thus, when one uses peak values of wall temperature or pitot pressure as indicative of transition location, they are defining a station approximately in the middle of the transition region. As shown in Refs. 1 and 2, the average point of transition determined by study of schlieren photographs usually lies close to the middle of the transition region too. In the remainder of this report, except where specifically noted, "transition location" is that station where  $p(x)/p_0$  was a maximum.

### 3.2 EFFECT OF LEADING-EDGE GEOMETRY

It is shown in Figs. 4 and 5 that increased leading-edge thickness, where  $b/x_t$  is very small, leads to higher Reynolds numbers of transition. This is not surprising in itself, the phenomenon having been demonstrated by earlier investigations (for example, Refs. 1, 4, 5, 7, and 8). However, the underlying cause is not clear. Moeckel (Ref. 9) has advanced a possible explanation, making the point that greater bluntness induces thicker entropy layers and correspondingly reduced local unit Reynolds numbers and Mach numbers near the surface. This hypothesis has been discussed in the light of experimental data in Ref. 5 with qualitative agreement indicated when  $x_t/b = 0(100)$ . Moeckel's flow model will be discussed later with respect to the present data.

The influence of bevel-angle\* indicated by the correlations in Refs. 1 and 2 for a Mach number of 3 also was investigated in the present case. The results are indicated in Fig. 6 where data are shown for the two cases corresponding to bevel angles of 5.6 and 12.5 deg. It is seen that any bevel-angle influence is negligible compared to the effect of leading-edge thickness. It should be noted here that the bevel-angle influence shown by the correlations of Refs. 1 and 2 was obtained by inclusion of data from several different wind tunnels, each one being associated with tests involving a different bevel angle. Since different wind tunnels were involved, it may be coincidental that the data correlated in terms of the bevel angles. The lack of a significant influence of bevel-angle in the present Mach 8 data suggests that the previous Mach 3 correlations should be reexamined on the basis of experiments in a single wind tunnel. Such was not within the scope of the present work but would be highly desirable for purposes of clarifying the issue regarding the interior bevel angle.

The influence of leading-edge thickness was evaluated with the aid of the present data, assuming any bevel-angle influence to be negligible. The data of Figs. 4 and 5 have been extrapolated to  $Re_b = 0$  for various constant unit Reynolds numbers as illustrated in Fig. 6, and the results are shown in Fig. 7. Also shown for comparison in Fig. 7 are the data for  $Re_b = 0$  from Refs. 1 and 2 for several Mach numbers. Again, as was the case for the lower Mach number data previously reported in Refs. 1 and 2, an effect of unit Reynolds number remains after attempting to eliminate the leading-edge thickness as a factor. It is also interesting to see that the large influence of Mach number on  $Re_{t, b = 0}$  indicated by the newer data for  $Re_b = 0$  is in keeping with the trend with Mach number shown by the earlier data for lower Mach numbers. It should be noted again that data from two different wind tunnels are included in Fig. 7.

The incremental increase in transition Reynolds number caused by nose bluntness has been evaluated by subtracting the  $Re_{t, b = 0}$  values as shown in Fig. 7 from the observed  $Re_t$  values, and the results are shown in Fig. 8. The data points of Fig. 8 represent measurements

---

\*This term is used herein to identify the apparent influence of the bevel angle at the leading edge on the side of the model opposite to the surface on which transition was measured in the several experiments referred to in Refs. 1 and 2. No explanation for this unexpected and possibly coincidental result has been established.

obtained from all six interchangeable noses and cover unit Reynolds numbers from  $0.1 \times 10^6$  to  $0.3 \times 10^6$  per inch; thus, the incremental increase in transition Reynolds number is seen to be dependent only on the bluntness Reynolds number,  $Re_b$ , for a given test Mach number. This result is the same as was previously found (Refs. 1 and 2) for the lower Mach number regime ( $3 \leq M_\infty \leq 5$ ).

### 3.3 INFLUENCE OF MACH NUMBER ON THE EFFECT OF BLUNTNESS

The growing effectiveness of nose bluntness in increasing the Reynolds number of transition,  $Re_t$ , with increasing Mach number is in qualitative agreement with Moeckel (Ref. 9). Moeckel has considered the reduced local unit Reynolds number caused by the shock wave created by a blunt nose and has suggested that transition moves downstream accordingly as nose thickness increases and causes more of the boundary layer to be occupied by low energy fluid which has passed through the strong part of the nose shock wave. If it is assumed that transition Reynolds number based on local flow properties in the boundary layer is unchanged by slight bluntness,  $Re_t$  (based on free-stream properties and wetted length,  $x_t$ , from stagnation point to transition) is increased when the local unit Reynolds number in the boundary layer is reduced by nose bluntness and associated shock losses in a layer of fluid near the surface of the body.

The incremental increase in transition Reynolds number caused by nose bluntness which was determined by the present experiment is shown in Fig. 8. Greater values of  $Re_b$  were investigated, but  $Re_t$  corresponding to these more blunt leading edges was so great that transition occurred downstream of the 68-in. -long body (for example, a test with  $Re_b = 4750$  and a unit Reynolds number of  $0.31 \times 10^6$  per in. results in  $Re_t > 21 \times 10^6$ ). Although the manner of presentation used in Fig. 8 is useful, it would be interesting to learn if the data can be collapsed to form a single curve by somehow accounting for the effect of varying Mach number, perhaps by means of Moeckel's theory.

A more direct comparison with Moeckel's theory can be made by considering the limiting case when the blunting is sufficiently great so that the Reynolds number at the outer edge of the laminar boundary-layer is close to the value at the surface of the blunted body in inviscid flow with otherwise identical conditions. From Moeckel's analysis, the range of bluntness Reynolds numbers,  $Re_b$ , for maximum influence

in the present case has been estimated as 2500 to 3300, depending on free-stream unit Reynolds numbers.\*

Using the transition Reynolds number extrapolated to  $Re_b = 0$  from Fig. 6 and the maximum local Reynolds number reduction (normal shock loss), limiting maximum  $Re_t/Re_t, b = 0$  can be computed by Moeckel's theory. Results of such estimates are shown as the curve labeled M. T. (1) in Figs. 9a and b. Shown for comparison in Figs. 9a and b are the experimental observations of  $Re_t$  corresponding to  $0 < Re_b < 3000$ , the extent of this experiment. It should be noted that  $Re_t$  did not, in the present experiments, reach a limit as  $Re_b$  increased (see Fig. 8).

Although reasonable agreement between the curve M. T. (1) and the data for finite  $Re_b$  is seen in the lower Mach number range, the Mach number influence is observed to be markedly less than that predicted by the theory. However, while Moeckel considered the reduced local Reynolds numbers created by the shock at the blunt leading edge, he did not consider the possible effect of the reduced local Mach numbers on boundary-layer transition. If it is assumed that the transition process is influenced by local Mach number near the outer edge of the boundary layer, or possibly at the height,  $Y_c$ , where maximum fluctuation energy was reported in Refs. 1 and 2, it follows that estimates of the influence of bluntness must involve an adjustment of, say  $Re_{t, b = 0}$ , to correspond to the inviscid, surface Mach number,  $M_n$ , rather than  $M_\infty$ . Obviously, when  $M_\infty \gg 1$ , then  $M_n \ll M_\infty$ , and the effect on  $Re_{t, b = 0}$  and  $Re_t$  may be large. Inasmuch as  $Y_c/\delta_t = 0.93$  under the conditions of the present experiments (for example, Fig. 14 of Ref. 1), there is no need to distinguish between  $Y_c$  or  $\delta_t$  as the important height to be matched by  $Y_n + \delta_t^*$  for maximum effect of bluntness when  $M_\infty \geq 8.0$  and  $T_w > 0.7 T_{aw}$ . Such is not the case when the lower Mach numbers of Fig. 9 are considered. For example, Ref. 1 shows  $Y_c/\delta_t = 0.66$  when  $M_\infty = 3.5$  and  $Y_c/\delta_t = 0.80$  when  $M_\infty = 4.5$ , where  $T_w = T_{aw}$  in both cases. But with  $\delta_t^*$  computed as in Ref. 10, it is found that  $\delta_t^* = Y_c$  at all Mach numbers in these experiments, and therefore  $Y_n + \delta_t^* = Y_c$  even for the smallest nose bluntness. Thus, in Fig. 9, the location of the low-energy layer, as it is defined by Moeckel, always lay between  $Y_c$  and  $\delta_t$ , even when  $b$  approached zero.

---

\*Larger values of  $Re_b$  are calculated for maximum effect if the estimate is based on measured boundary-layer thickness instead of the theoretical thickness because the latter generally is less than the measured  $\delta_t$ . However, it being the intention to follow Moeckel in all respects, the required  $Re_b$  is computed by use of his equations.

The values of  $Re_{t, b=0}$  at each Mach number in Fig. 9 were multiplied by Moeckel's factor  $(Re_n/Re_1)^{-1}$  to obtain the curve M. T. (1). The curve M. T. (2) was obtained by reducing  $Re_{t, b=0}$  at a particular  $M_\infty$  to the value of  $Re_{t, b=0}$  given for  $M_n = f(M_\infty)$ . Thus, for example, when  $M_\infty = 8$  and  $U_\infty/\nu_\infty = 10^5 \text{ in.}^{-1}$ ,  $Re_{t, b=0} = 4.5 \times 10^6$ ,  $Re_n/Re_1 = 0.086$  and  $M_n = 3.56$ . This leads to  $Re_t$  on curve M. T. (1) being  $11.6$   $Re_{t, b=0} = 5.2 \times 10^7$ . On curve M. T. (2) the corresponding ordinate is

$$\begin{aligned} Re_t &= 5.2 \times 10^7 \frac{Re_{t, b=0} \text{ for } M = M_n = 3.56}{Re_{t, b=0} \text{ for } M = 8} \\ &= 5.2 \times 10^7 \times 0.189 = 9.9 \times 10^6 \end{aligned}$$

Note that  $Re_{t, b=0} = f(M_\infty, U_\infty/\nu_\infty)$

Implications regarding Moeckel's flow model, while not entirely conclusive, are not favorable because the experimental data show that  $Re_t$  continued to increase and yet was well short of the theoretical maximum as  $Re_b$  approached the value for which a maximum  $Re_t$  was calculated by Moeckel's method.\* Also, the measured boundary-layer pitot-pressure profiles showed no discernible layer of reduced Mach number at or near the outer edge of the boundary layer. When considering the present, typical cases, it becomes difficult to accept the idea that a layer of reduced unit Reynolds number having a thickness  $Y_n \approx \delta_t/40$  could influence transition location to the extent observed.

#### 4.0 CONCLUDING REMARKS

The influence of leading-edge geometry on boundary-layer transition has been studied under hypersonic ( $M_\infty = 8$ ) flow conditions and the following observations are made:

1. Contrary to the outcome of earlier studies of leading-edge geometry (Refs. 1 and 2), an influence of the lower or interior bevel angle of a finite leading edge was not found in the present studies. The previous studies considered data from several different supersonic wind tunnels, each bevel angle corresponding to tests conducted in a different tunnel. It is suggested that the previously indicated bevel-angle influence at lower supersonic speeds should be experimentally studied in a single wind tunnel, as is the case with the data presented herein.

---

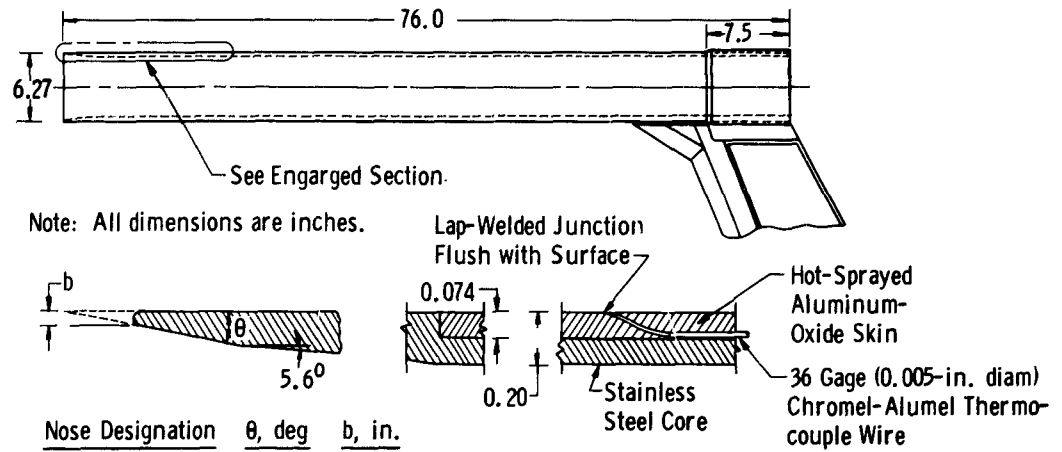
\*It is interesting to note that the data of Ref. 11, for  $2 \leq M_\infty \leq 4$ , show  $Re_t$  continuing to increase where  $Re_b = 10^5$  and  $M_\infty \geq 3$ .

2. In keeping with the previous studies at lower supersonic speeds, the data for  $M_\infty = 8$  indicate an incremental increase in transition Reynolds number which is, for a given Mach number, a function only of a Reynolds number based on the leading-edge thickness.
3. An approximation to "sharp" or "aerodynamic" flat-plate transition Reynolds numbers is obtained by extrapolation of the present data to zero bluntness Reynolds number, and, again in keeping with the previous studies, a unit Reynolds number influence on the transition Reynolds number remains.
4. Comparison of the leading-edge bluntness influences derived from the present Mach 8 and previous Mach 3 to 5 data with the theoretical flow model according to Moeckel indicates qualitative agreement; however, the quantitative influence of Mach number is not predicted by Moeckel's theory. Whether Moeckel's hypothesis that the change in transition Reynolds number caused by leading-edge bluntness is due entirely to a reduced local unit Reynolds number or whether more subtle changes in the stability of the laminar boundary layer are effected by slight leading-edge bluntness cannot be established at the present time. Thus, data presented in the form of Fig. 8 appear to offer the better means now available for evaluating the effect of small degrees of leading-edge bluntness.

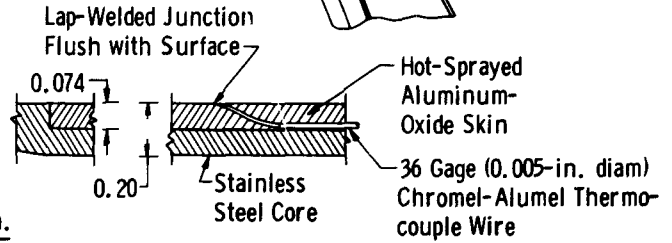
#### REFERENCES

1. Potter, J. Leith and Whitfield, Jack D. "Effects of Slight Nose Bluntness and Roughness on Boundary-Layer Transition in Supersonic Flows." Journal of Fluid Mechanics, Vol. 12, Part 4, pp. 501-535, April 1962.
2. Potter, J. Leith and Whitfield, Jack D. "Effects of Unit Reynolds Number, Nose Bluntness, and Roughness on Boundary Layer Transition." AEDC-TR-60-5, March 1960.
3. Potter, J. Leith and Durand, Jack A. "Analysis of Very Thick Laminar Boundary Layers in Axisymmetric High-Speed Fluid Flow." Developments in Theoretical and Applied Mechanics, Vol. 1, Plenum Press, New York, 1963, pp. 341-360.
4. Rogers, Ruth H. "Boundary Layer Development in Supersonic Shear Flow." AGARD Rept. 269, April 1960.

5. Brinich, Paul F. and Sands, Norman. "Effect of Bluntness on Transition for a Cone and a Hollow Cylinder at Mach 3.1." NACA TN 3979, May 1957.
6. Sivells, James C. "Operational Experience with a 50-Inch Diameter Mach 8 Tunnel." Paper presented at STA-AGARD Wind Tunnel and Model Testing Panel, Marseille, France, 1959.
7. Bertram, Mitchel H. "Exploratory Investigation of Boundary-Layer Transition on a Hollow Cylinder at a Mach Number of 6.9." NACA TR 1313, 1957. (Supersedes NACA TN 3546, 1959.)
8. Brinich, Paul F. and Diaconis, Nick S. "Boundary-Layer Development and Skin Friction at Mach 3.05." NACA TN 2742, July 1952.
9. Moeckel, W. E. "Some Effects of Bluntness on Boundary-Layer Transition and Heat Transfer at Supersonic Speeds." NACA TN 3653, March 1956.
10. Cohen, C. B. and Reshotko, E. "The Compressible Laminar Boundary Layer with Heat Transfer and Arbitrary Pressure Gradient." NACA Report 1294, 1956.
11. Jillie, Don W. and Hopkins, E. J. "Effects of Mach Number, Leading-Edge Bluntness, and Sweep on Boundary-Layer Transition on a Flat Plate." NASA TN D-1071, September 1961.



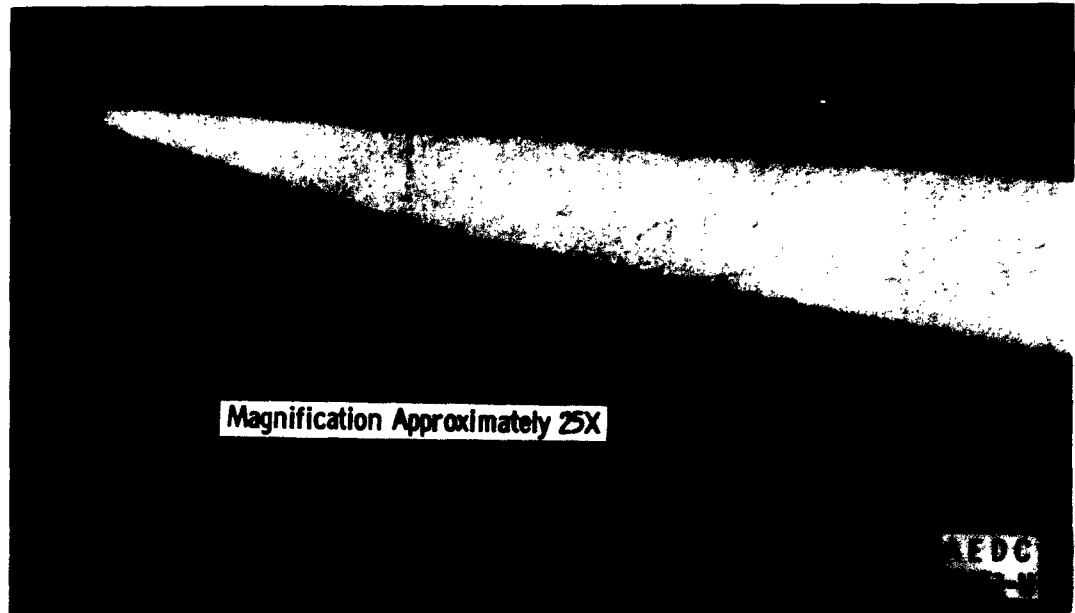
Note: All dimensions are inches.



Nose Designation	$\theta$ , deg	b, in.
N <sub>1A</sub> (Ref. 1)	12.9	0.0006
N <sub>2A</sub>	12.7	0.0034
N <sub>3A</sub>	12.2	0.0067
N <sub>4A</sub>	12.0	0.0094
N <sub>2B</sub>	5.2	0.0032
N <sub>3B</sub>	6.1	0.0064

$\bar{\theta} = 12.5 \text{ deg}$   
 $\bar{\theta} = 5.6 \text{ deg}$

a. The 6-in.-diam, Hollow Cylinder Model



b. Enlarged Photograph of Cross Section of Typical Model Leading Edge

Fig. 1 Typical Models

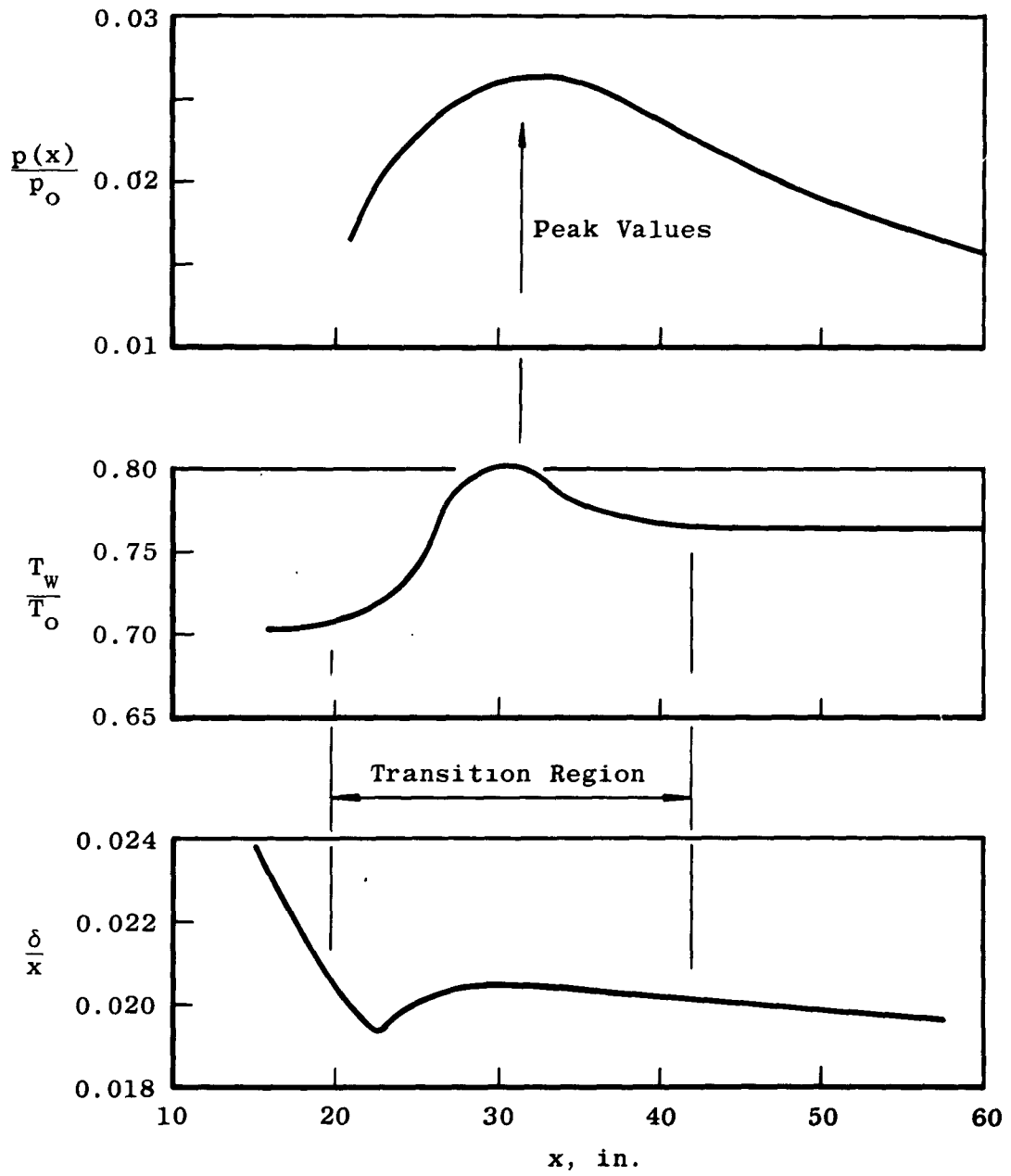


Fig. 2 Typical Data Showing Location of Boundary-Layer Transition on Hollow Cylinder at  $M_\infty = 8$

Basis of Location

- ◇  $\delta \sim x^{1/2}$  End of laminar flow
- △  $\delta \sim x^{4/5}$  Beginning of turbulent flow
- ▽  $T_w = \text{Maximum}$
- ▽  $T_w = \text{Constant at turbulent level}$
- $p(x) = \text{Maximum}$

Note: Filled symbols denote new data.  
 Open symbols are data of Refs. 1 and 2.

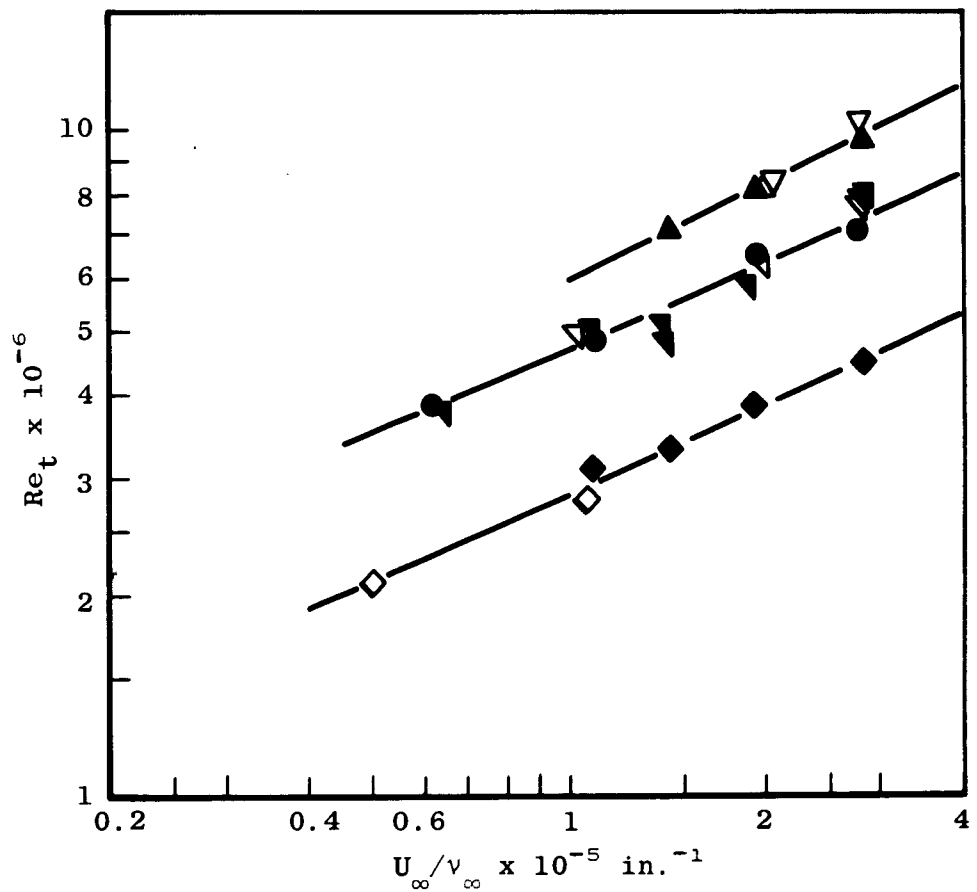


Fig. 3 Reynolds Number of Transition on Hollow Cylinder at  $M_\infty = 8$   
 with  $b = 0.0006 \text{ in.}$  and  $\bar{\theta} = 12.5 \text{ deg}$

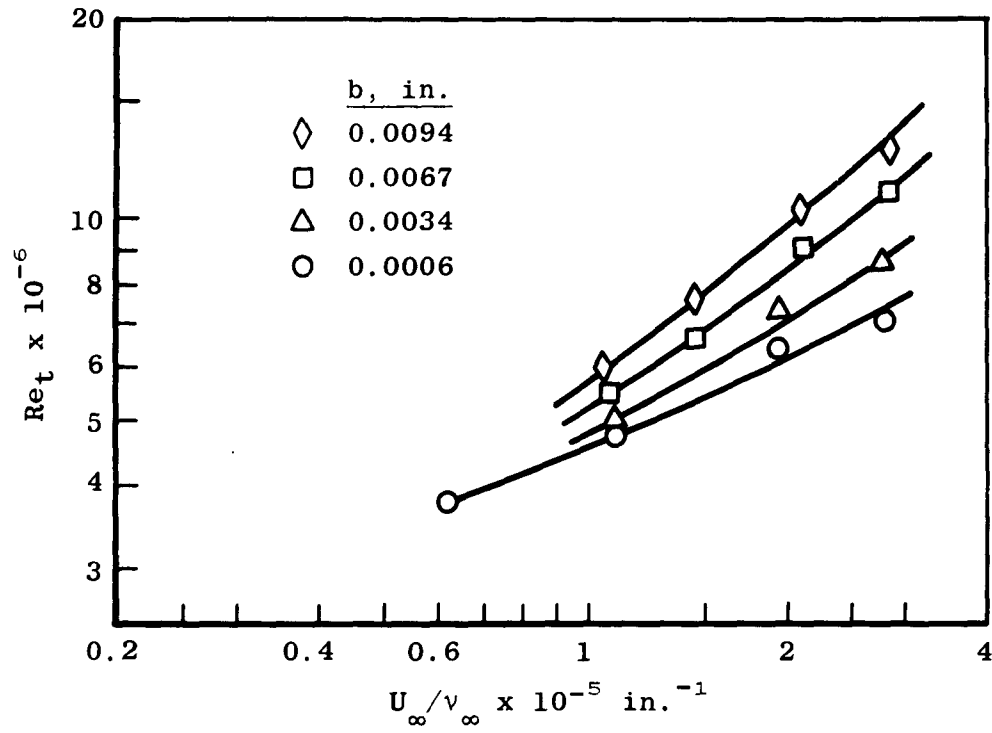


Fig. 4 Basic Data Showing  $Re_t$  as a Function of  $U_\infty/v_\infty$  and  $b$  for  $M_\infty = 8$  and  $\bar{\theta} = 12.5$  deg

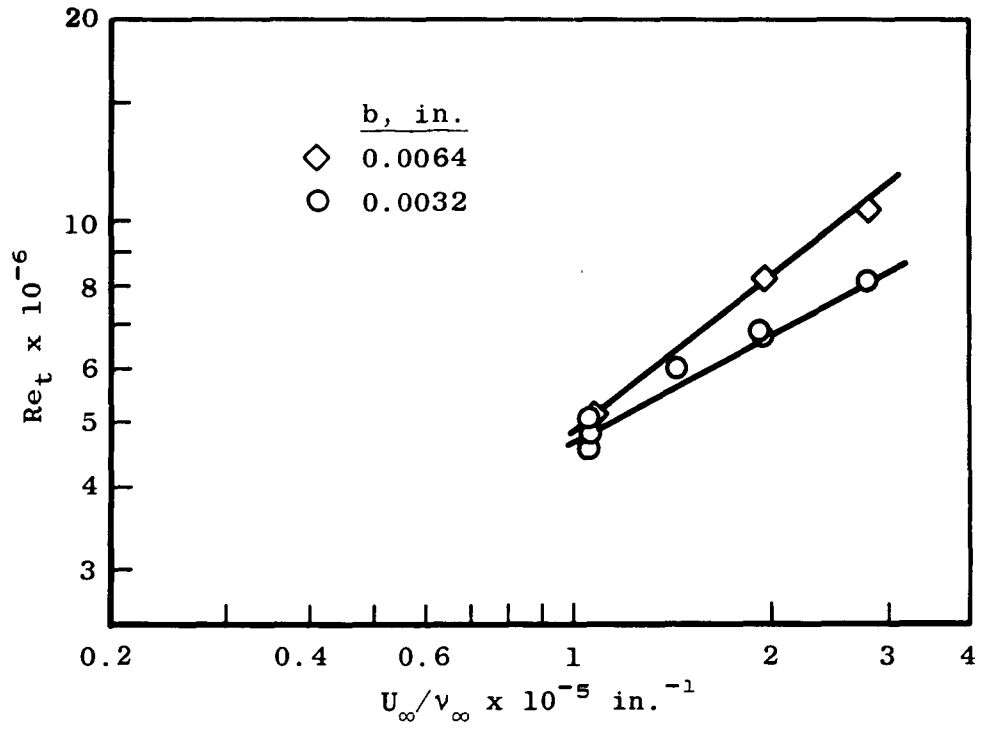


Fig. 5 Basic Data Showing  $Re_t$  as a Function of  $U_\infty/v_\infty$  and  $b$  for  $M_\infty = 8$  and  $\bar{\theta} = 5.6$  deg

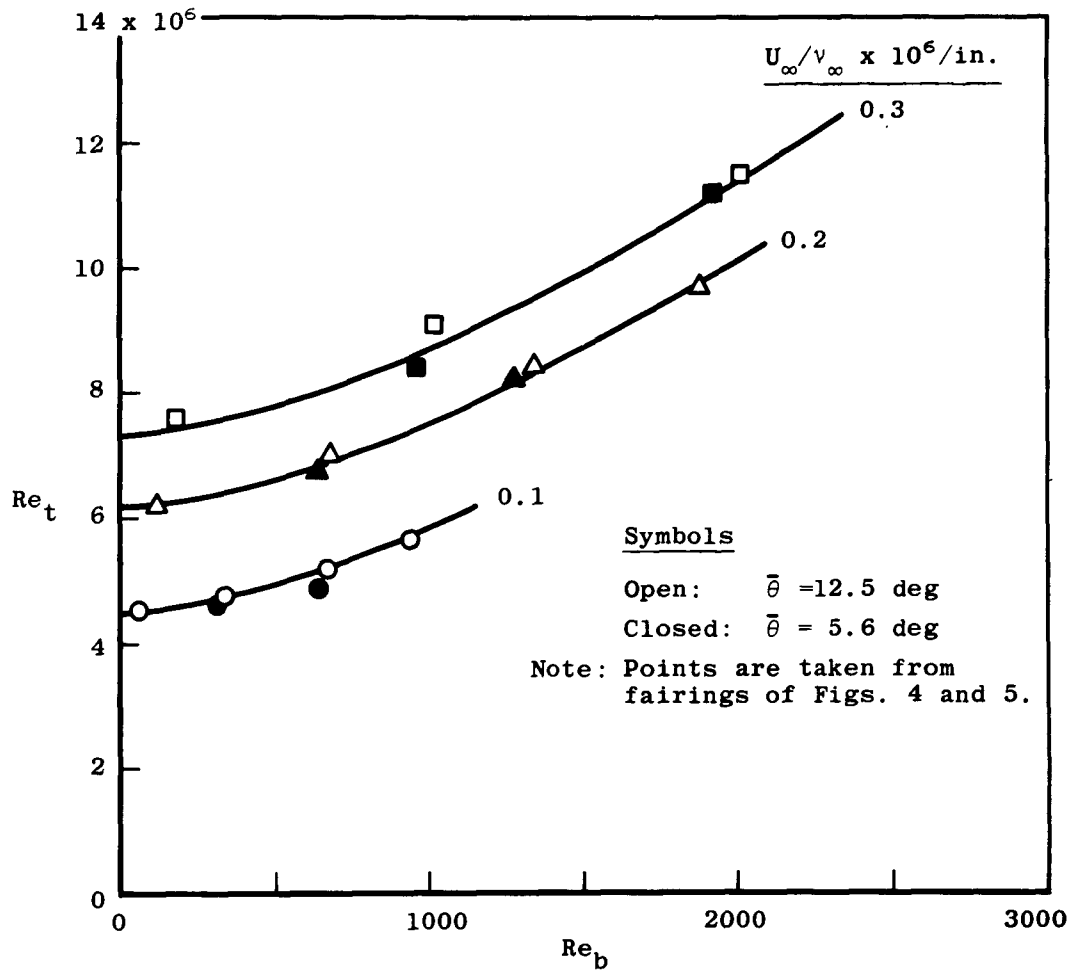


Fig. 6 Bluntness Reynolds Number Influence for Various Unit Reynolds Numbers

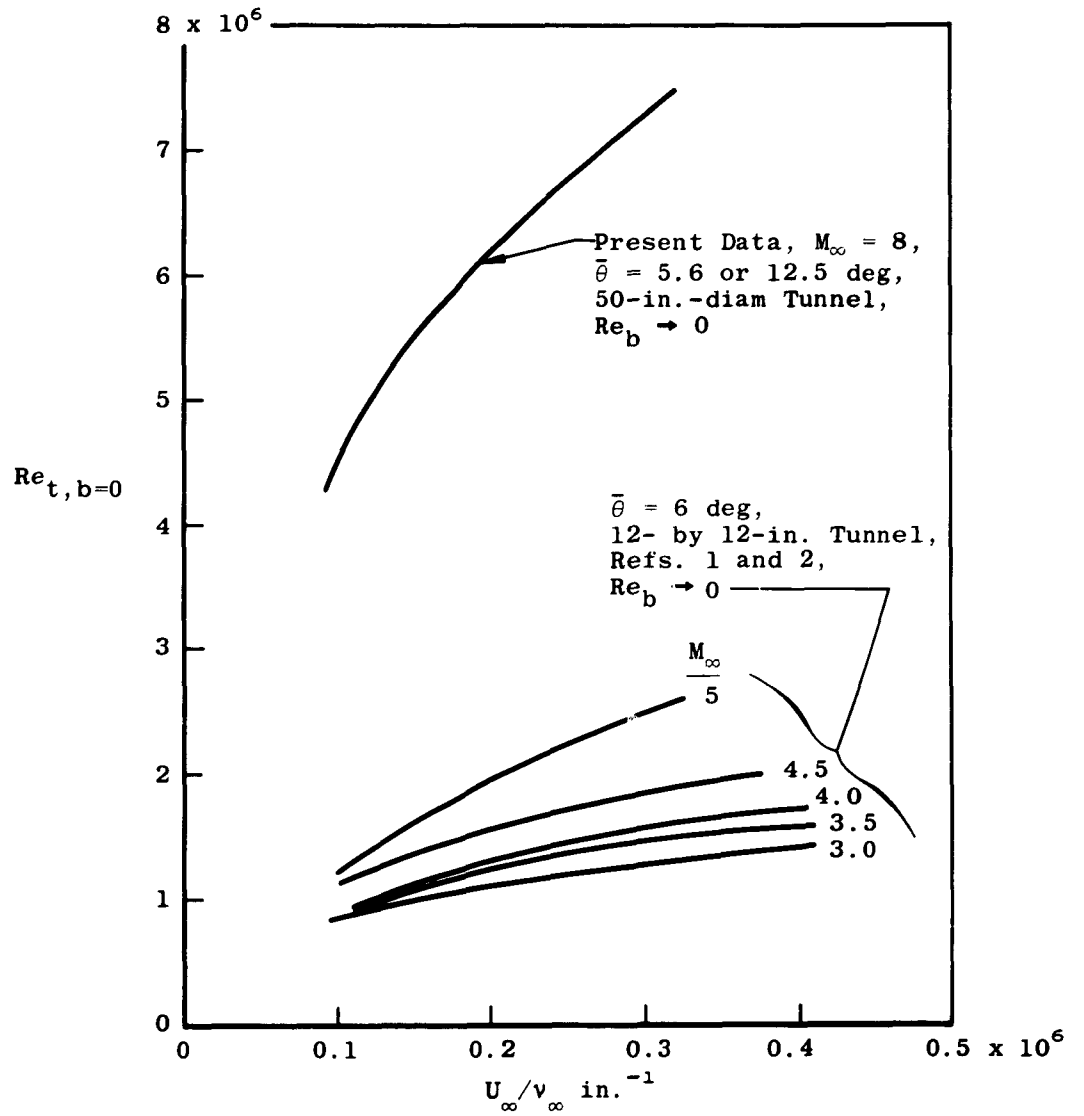


Fig. 7 Unit Reynolds Number Effect for Various Mach Numbers as  $Re_b \rightarrow 0$

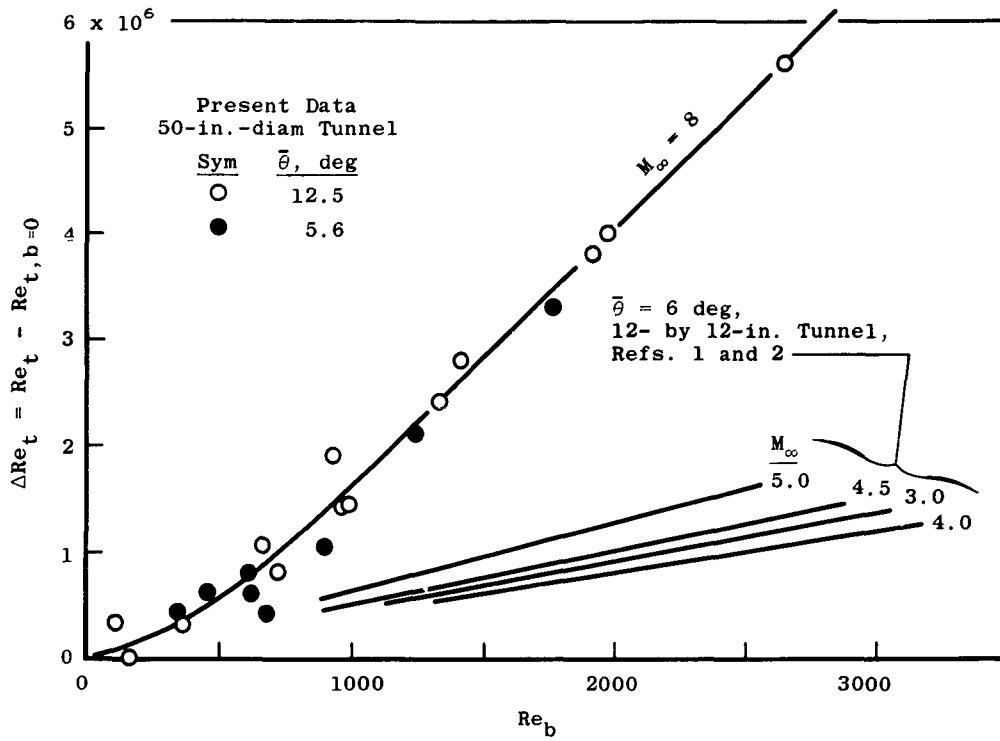


Fig. 8 Transition Reynolds Number Increase as a Function of Bluntness Reynolds Number

- E. D. ( $Re_b = 0$ ) Experimental data extrapolated to  $Re_b = 0$ 
    - $\bar{\theta} \approx 6$  deg, Refs. 1 or 2, experiment
    - ▲  $\bar{\theta} \approx 5.6$  or  $12.5$  deg, present experiment
  - M. T. (1) Moeckel theory for maximum effect of bluntness (Ref. 9) using experimental data of Refs. 1 and this report for  $Re_{t,b=0}$
  - M. T. (2) As in M. T. (1) but with reduced local Mach number,  $M_n$ , replacing  $M_\infty$  in determining  $Re_{t,b=0}$
- Shaded bars indicate experimental data for  $0 < Re_b < 3000$

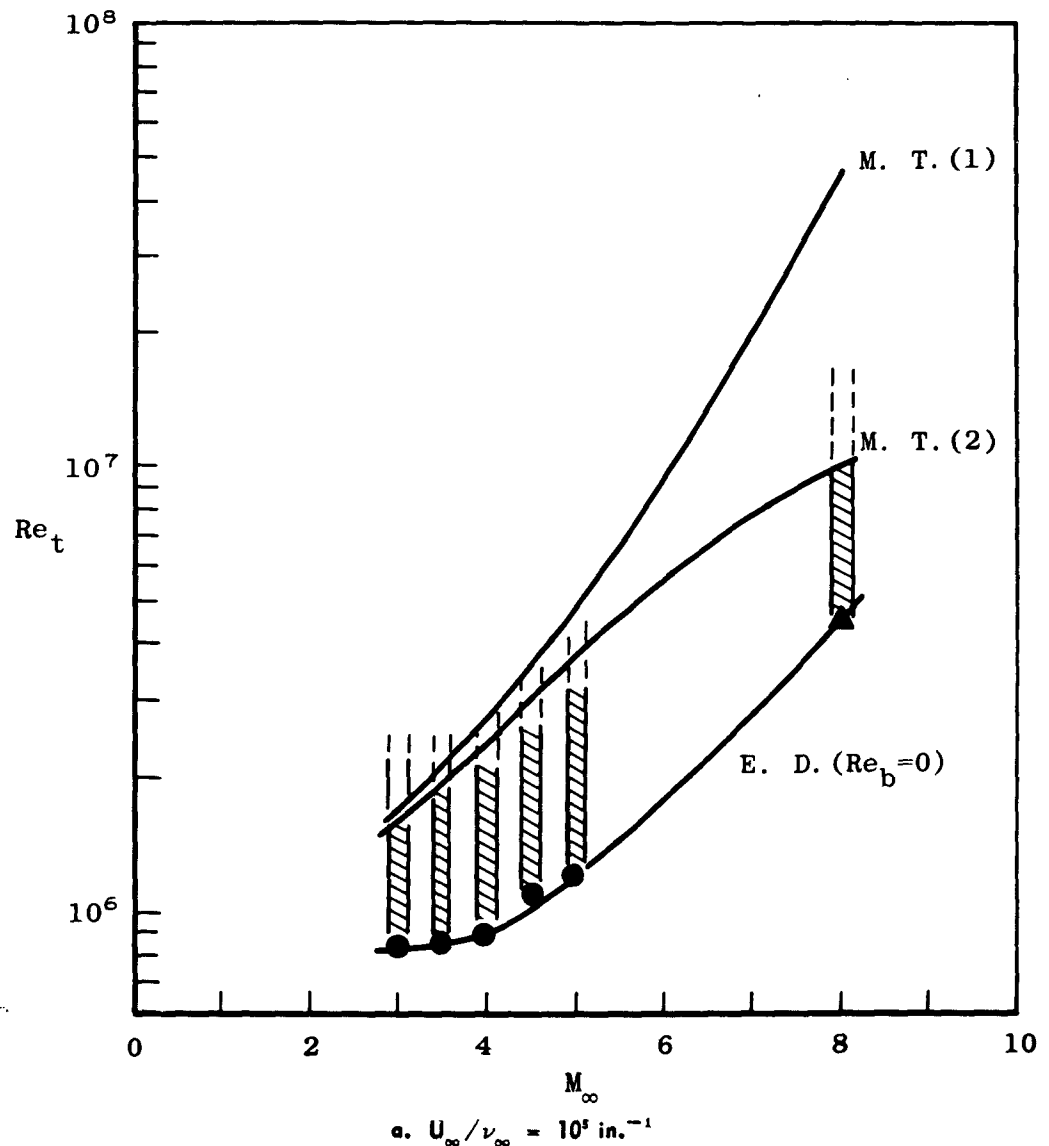
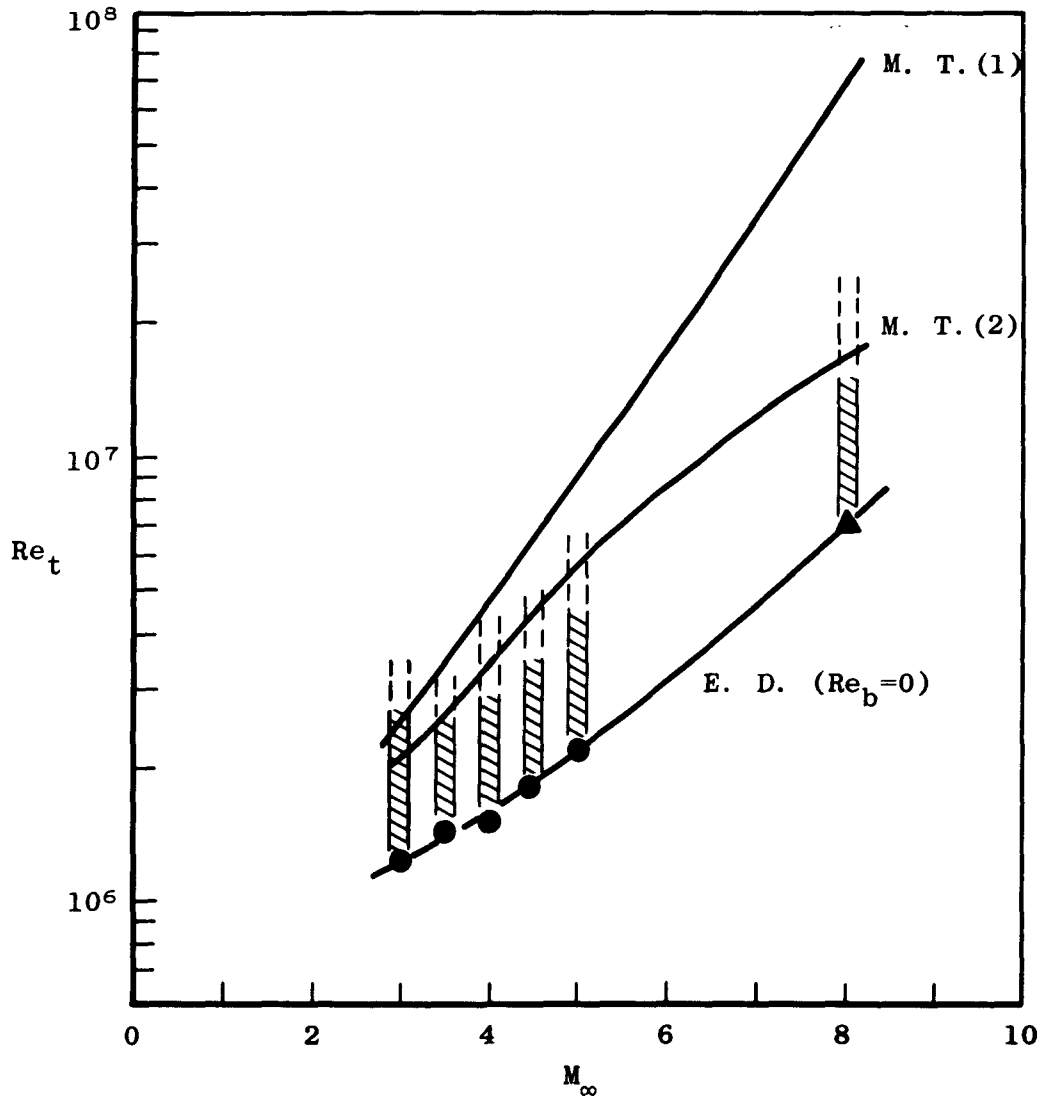


Fig. 9 Comparison of Experiment and Theory for Mach Number Influence on Bluntness Effect

- E. D. ( $Re_b = 0$ ) Experimental data extrapolated to  $Re_b = 0$ 
    - $\bar{\theta} \approx 6$  deg, Refs. 1 or 2, experiment
    - ▲  $\bar{\theta} \approx 5.6$  or  $12.5$  deg, present experiment
  - M. T. (1) Moeckel theory for maximum effect of bluntness, Ref. 9, using experimental data of Refs. 1 and this report for  $Re_{t,b=0}$
  - M. T. (2) As in M. T. (1) but with reduced local Mach number,  $M_n$ , replacing  $M_\infty$  in determining  $Re_{t,b=0}$
- Shaded bars indicate experimental data for  $0 < Re_b < 3000$



b.  $U_\infty / \nu_\infty = 3 \times 10^5 \text{ in.}^{-1}$

Fig. 9 Concluded